Int. J. Electrochem. Sci., 15 **(2020)** 3469 – 3478, doi: 10.20964/2020.04.57

International Journal of
ELECTROCHEMICAL
SCIENCE
www.electrochemsci.org

Controllable Synthesis of Silver Nanoparticles by the Pulsed Electrochemical Deposition in a Forced circulation Reactor

Di Yin[1], *Yiyang Liu*[1], *Peng Chen*[1], *Guangyuan Meng*[1], *Guangtuan Huang*[1], *Lankun Cai*[1], *Lehua Zhang*[1,2,*]

[1] State Environmental Protection Key Laboratory of Environmental Risk Assessment and Control on Chemical Process, School of Resources and Environmental Engineering, East China University of Science and Technology, Shanghai 200237, P. R. China.
[2] Shanghai Institute of Pollution Control and Ecological Security, Shanghai 200092, P. R. China.
[*]E-mail: lezhanghua@163.com

Received: 26 December 2019 / *Accepted:* 210 February 2020 / *Published:* 10 March 2020

A novel pulsed electrochemical system was constructed to synthesize size-controllable spherical AgNPs in the aqueous phase. The circulation system was found to greatly reduce silver deposition rate, thereby making well-dispersed AgNPs colloids to be synthesized very convenient without ultrasonication and string system. Moreover, the particle size of AgNPs were controlled by the experimental parameters (on-time, off-time, and peak current) to improve homogeneity of the prepared AgNPs. The smallest sized AgNPs with a size of 14.9±4 nm were obtained with an on-time, off-time, and peak current of 0.8 ms, 0.3 ms, and 0.2 A, respectively. In addition, a clear linear positive correlation between the size of silver nanoparticles and the peak current was found in this system.

Keywords: Silver nanoparticles; Controllable synthesis; Pulsed electrochemical system

1. INTRODUCTION

In recent years, metal nanoparticles have attracted substantial interests in numerous fields. In particular, silver nanoparticles (AgNPs) have been widely used in catalysis [1, 2], anti-bacterial materials [3], sensors [4], superconductors [5] and optics [6, 7] owing to their unique characteristics, including high catalytic activities, conductivities and electrochemical activities. Moreover, it is well known that the distribution, morphology and size of silver nanoparticles affects their properties in physical and chemical reactions, especially in optical, magnetic and electrochemical applications [8].

A lot of methods have been proposed and developed to prepare AgNPs such as gamma irradiation [9], chemical reduction [10], photoreduction [11, 12], microwave processing [13], electrochemical methods [14, 15] and sonoelectrochemical methods [16, 17]. Among this, electrochemical methods are rapid, environmentally friendly and it can also achieve precise particle-size control by adjusting the current density directly without a need for vacuumor expensive equipment. So, it has been widely used to synthesize silver nanoparticles [18]. Well-defined AgNPs have been prepared by wrapping with low-density polyethylene on a carbon rod [19]. Ikhsan et al. prepared reduced graphene oxide supported AgNPs via the electrochemical method, and the composite could be used for the detection of 4-nitrophenol [20]. Moreover, Xia Qin et al. [21] and Yan et al. [22] indicated that the morphology and size of AgNPs can be controlled by many electrochemical parameters, such as frequency, on- and off-times, duty cycle. In contrast with the direct current electrochemical method, the pulse electrochemical method is a versatile method that is very convenient for adjusting reaction conditions. As pointed out before all of electrochemical methods exist one limitation is that AgNPs can be covered on the cathode more easily during the electrochemical process, so it is difficult to produce AgNPs in aqueous phase. Especially, the particle production comes to a halt altogether when the entire cathode surface coated with the silver electrodeposits. The addition of poly (N-vinylpyrrolidone) (PVP), which was first introduced by Yin et al. and involves adjusting electrolysis parameters, has been employed to prepare size-controlled and well-dispersed silver nanoparticles in aqueous medium. In this condition, intensive stirring during the process of electrolysis was also needed to inhibit the formation of precipitates [23]. Mechanical stirring transferred the nanoparticles effectively from the electrode surface to the main solution, which are conducive to the uniform growth of AgNPs. However, the self-vibration of AgNPs and the collision contact with cathode in the layer liquid near the electrode interface cannot weaken. So some of those AgNPs may get the negative charge from cathode during the process of collision. Then the charged AgNPs behave like the cathode, which cause the reduction of silver ions on its surface and the growth of original AgNPs [24, 25]. A feasible and practical technology is urgently needed for the synthesis of AgNPs colloids with homogeneous morphology [26].

In this study, we developed an easier and more effective circulation pulsed electrochemical system to synthesize well-dispersed and size-controlled AgNPs colloids. Compared to ultrasonication and string system, circulation is better at reducing the silver deposition on cathode. Because it can not only transfer the nanoparticles from the electrode surface to the main solution, but also reduced the collision of AgNPs and the electrode so that a few of AgNPs would be charged and the number of the aggregated large-particle silver decreased. The effect of different electrochemical parameters (on-time, off-time, peak current density) of this system on the size of AgNPs was then investigated. AgNPs colloids was thoroughly analysed by Malvern spray analyzer, FE-SEM (Field Emission - Scanning Electron Microscope), EDS (Energy Dispersive Spectrometer) and XRD (X-ray Diffraction).

2. EXPERIMENTAL

2.1 Materials and characterization

Ultra-pure deionized (DI) water (>18.2 MΩcm) was used throughout this study. Silver nitrate ($AgNO_3$), poly(N-vinylpyrrolidone) (PVP-K30, average molecular weight of approximately 40,000) and ethanol (C_2H_5OH) were of analytical grade and used without further purification. Silver sheets were purchased from Baoji Chuangqi metal Co., Ltd. (Baoji, China). The conductivity of the deionized water used was less than 0.05 μS/cm.

A Malvern spray analyzer (Zetasizer Nano, Malvern Panalytical, UK) was used to investigate the sizes of the silver nanoparticles. Field-emission scanning electron microscopy (FESEM, Sigma 300, Zeiss, Germany) equipped with energy dispersive X-ray spectroscopy (EDS, Falcon, EDAX, USA) was employed for distribution, morphological and elemental analysis of the silver nanoparticles. X-ray diffraction (XRD, D/max2550 V Rigaku, Japan) was used for phase analysis. A 20 mL silver nanoparticle colloidal solution was prepared after the reaction by centrifuging 3 times at a rotational speed of 9000 rpm for 20 min. Then, 20 mL of ethanol was added to the samples before subsequent centrifugations, and the supernatant was discarded after each centrifugation step. After centrifugation, the AgNPs were dispersed in deionized water. Two drops of silver nanoparticles colloidal solution were dehydrated on the surface of aluminum foil for SEM analyze.

2.2 Preparation of the AgNPs

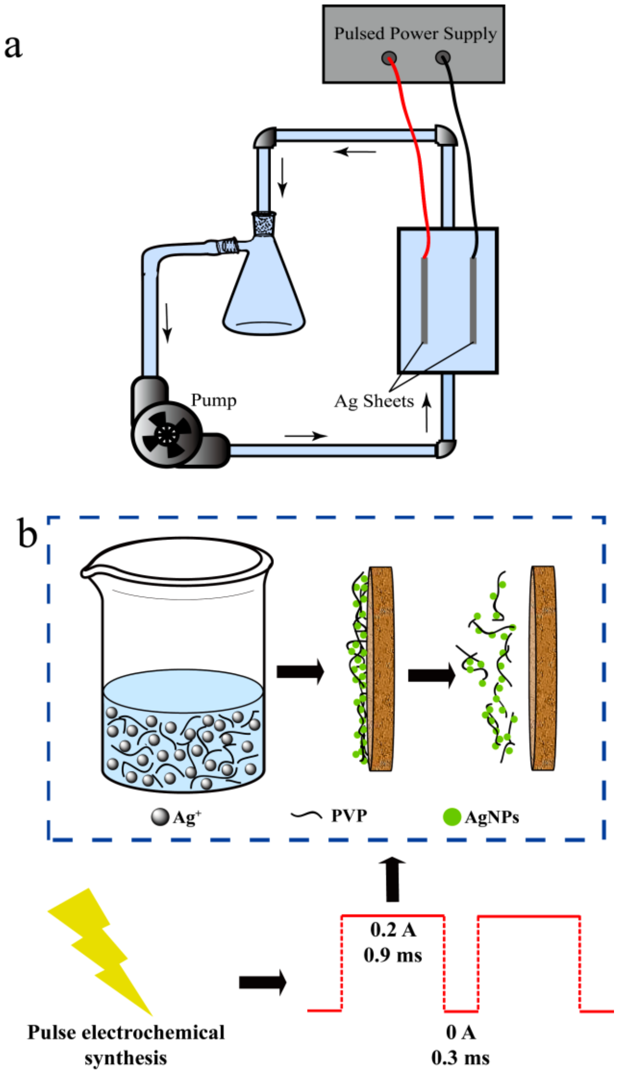

Figure 1. Schematic diagramof the prepared AgNPs: (a) the circulation pulsed electrochemical system to prepare AgNPs. (b) the formation process of AgNPs on this system.

Two silver electrode sheets were used as the working electrode in turn as the electrode polarity changed every 30s, and the electrode area was 3 cm^2 (2 cm*1.5 cm). A 500 mL reaction solution of 2 g/L $AgNO_3$ was circulated at 6 L/min, and the reaction time was 30 min (Figure 1 (a)). A pulsed current was generated by a DC pulse output (MCUB-2010C, CNDHE, China) with periodic reversal of the polarity (2 times per minute) and 10 g/L PVP was added to the aqueous system before the reaction to reduce the particle size [23]. The on-time and off-time were adjusted by changing the frequency and duty cycle. The reaction of the prepared AgNPs for characterization was 30 min at 0.2 A with an on-time of 0.9 ms, an off-time of 0.3 ms. The off-time was set to 0.3 ms, and the on-time was adjusted from 0.1 to 0.9 ms in the on-time experiments; similarly, the on-time was set to 0.3 ms, and the off-time was adjusted from 0.1 to 0.9 ms in the off-time experiments. The peak current was set to 0.2 A (i.e., 67 mA/cm^2) in the on-time and off-time experiments, which is higher than that used for the routine direct current deposition of silver because the characteristics of the pulsed electrochemical result in the production of smaller-sized nanoparticles at the same current density [27]. In the size-controllable experiment, the on-time was set to 0.9 ms and the off-time was set to 0.3 ms, and the peak current was adjusted from 0.05 A to 0.5 A (i.e., 16.7 mA/cm^2 to 167 mA/cm^2). The silver nanoparticles, which were prepared in an aqueous solution, were washed with ethanol to remove the PVP from the colloidal solution. The synthesis mechanism of silver particles in this electrochemical system is generally proposed on the basis of three steps simply, as is shown in Figure 1 (b). The first step is the formation of coordinative bonding between silver ions and PVP. Because PVP has a structure of a polyvinyl skeleton with polar groups, silver ions can anchor at a PVP molecule and producing the Ag_m^{m+}–PVP complex (m is the number of silver ions). The second step is the Ag_m^{m+}–PVP complex migration to the cathode interface and reductive formation of Ag_m^0–PVP. The last step is the separation of Ag_m^0 –PVP from the cathode and their further migration caused by the flow of solution [23].

3. RESULTS AND DISCUSSION

3.1 Characterization of AgNPs

Synthesized AgNPs using the novel pulsed electrochemical system were thoroughly characterized using SEM, EDS and XRD to determine particle morphology and crystallinity. The morphology of the prepared AgNPs were investigated using SEM (Figure 2). As shown in Figure 2 (a), AgNPs were spherically and well dispersed with a diameter range of 10–30 nm, and few of the AgNPs showed large size due to the aggregation of AgNPs. Figure 2 (b) shows the surface morphology of the silver electrode after reaction. After 30 min reaction, a number of nanoparticles were deposited on the electrode. However, the nanoparticles that were deposited on the electrode were not of uniform size, which indicated three-step mechanism. The nanoparticles were deposited on the electrode first before being stripped into the aqueous solution. Compared to other researches [23, 28], the depositon of AgNPs on the electrode are lower than other papers, especially under the condition of high current and long reaction time. To confirm the composition, EDS spectra (Figure 2 (c)) carried out, indicating that the elemental compositions of two samples prepared at peak currents of 0.2 A with Ag and O found to be the most abundant elements in the samples. The molar fractions of silver and oxygen in the sample prepared were 94.95% and 5.05%, respectively. For the synthesis of AgNPs with PVP, the PVP first complexed with Ag^+, and the complicated dendritic morphology prevented epitaxial growth of the AgNPs; thus, the AgNPs were coated with PVP after the reaction. The EDS results show that after repeated washing with ethanol and water, the PVP dispersant could be removed. XRD was carried out to find the crystallinity of AgNPs prepared with peak current of 0.2 A. XRD measurements (Figure 2 (d)) of the product showed that Ag formed since the characteristic peaks were well matched with those from the standard pattern; the peaks at 38.2°, 44.5°, 64.6° zand 77.58° were matched to the (111), (200), (220), and (311) facets of face-centered cubic (FCC) structure of AgNPs. The values agreed with Joint Committee on Powder Diffraction (JCPD, standard file no. 04-0783). The peak of XRD broadened apparently because of the small size of AgNPs (5–25 nm) [29, 30]. Peaks for other materials, such as Ag_2O, were hard to find, indicating the high purity of the silver particles.

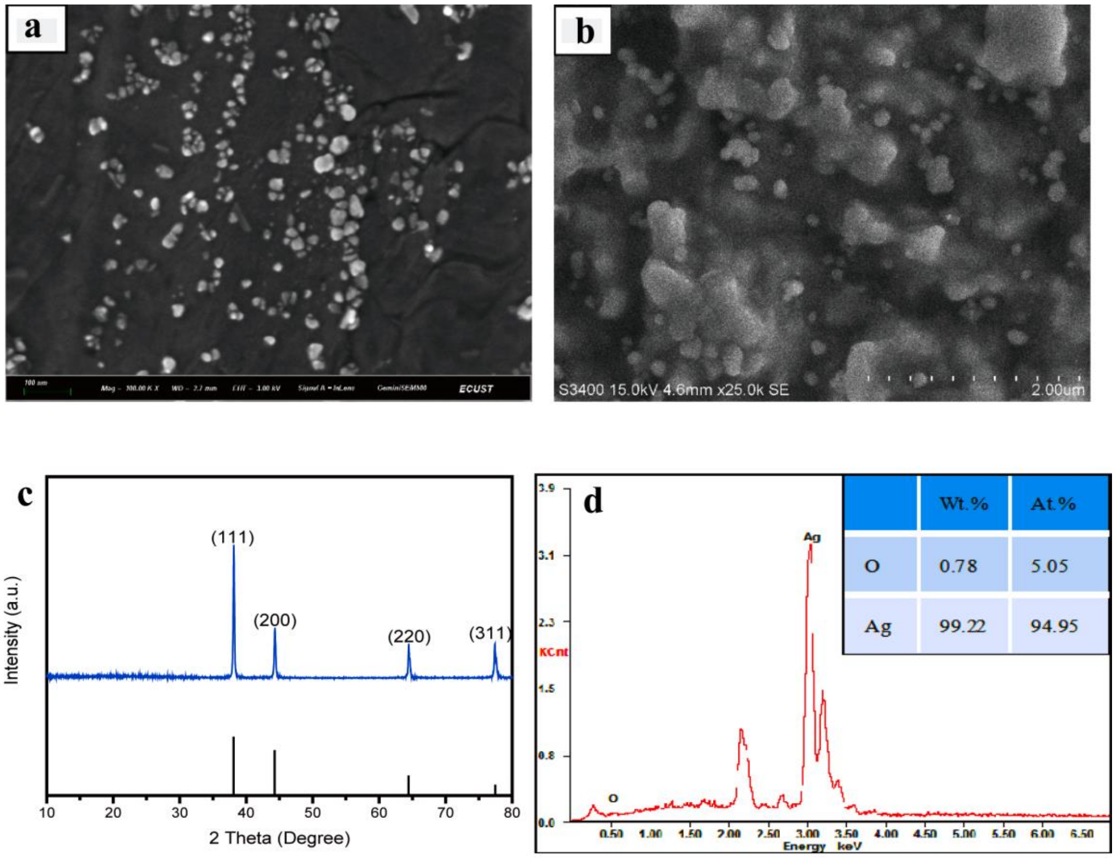

Figure 2. Characterization of the prepared AgNPs: SEM images of AgNPs in the solution (a) and on the electrode (b) after 30 min reaction at 0.2 A with an on-time of 0.9 ms, an off-time of 0.3 ms, and a PVP concentration of 10 g/L. The main elements were Ag and O of energy dispersive X-ray spectroscopy (EDS) (c) of the prepared AgNPs. X-ray diffraction (XRD) (d) of the prepared AgNPs.

3.2. Effect of the on-time and off-time on the size of AgNPs

To investigate the effect of the on-time on the size of AgNPs, the corresponding frequency and duty cycle were set in the first group of experiments to maintain an off-time of 0.3 ms, and the on-time was adjusted from 0.1 ms to 0.9 ms. In these measurements, the off-time was 0.3 ms, and the peak current was 0.2 A. The sizes of the AgNPs in these samples are shown in Figure 3 (a). The particle size was influenced by the on-time of the reaction. When the on-time was less than 0.2 ms, the particle size increased with increasing on-time. The particle size peaked at 26.3±2.1 nm when the on-time was 0.2 ms. However, as the on-time continued to increase, the size of the particles decreased until reaching an on-time of 0.7 ms; the size of the particles for on-times ranging from 0.7 to 0.9 ms was approximately flat. The on-time is a direct factor for the particle size in a pulsed electrochemical system. In a pulsed electrochemical system, the silver crystals have a longer growth time with increasing reaction time; thus, the size of the nanoparticles are larger, which is consistent with the results from previous research [21]. However, excessively long reaction times produced the opposite results, and the reaction was controlled by Ag diffusion. When the current was applied, the concentration of Ag on the surface of the cathode rapidly decreased. As the reaction times was longer but pulse intervals were invariant, the concentration of silver on the surface of electrode maintained in a lower level, which caused the smaller size of products. Moreover, the coordinative bonding between silver ions and PVP (Ag_m^{m+}–PVP) was well developed as the on-time increased and the formation of Ag_m^{m+}–PVP complex was able to prevent the agglomeration of AgNPs [16, 31].

In the pulsed electrochemical system, the effect of off-time was mainly attributed to the compensation speed of ions on the electrode surface [32]. Figure 3 (b) shows the particles sizes for varying off-times. In these measurements, when the on-time was set to 0.3 ms, the sizes of the AgNPs produced with varying off-times were relatively small, the influence of the off-time was less than that of the on-time. The particle sizes for off-time longer than 0.3 ms were larger than those for off-times shorter than 0.3 ms. In theory, the longer the off-time, the larger the size of AgNPs due to the Ag^+ compensation on the electrode surface [27]. Ions consumed during the on-time can be completely replenished during a longer off-time, which leads to larger sizes. In this system, the solution was circulated at 6 L/min (the theoretical velocity of the flow was 0.67 m/s) to transfer AgNPs from the electrode surface to the main solution, hence, the agglomeration of AgNPs could be avoided under different off-times and off-time had less effect on the size of the prepared AgNPs [33].

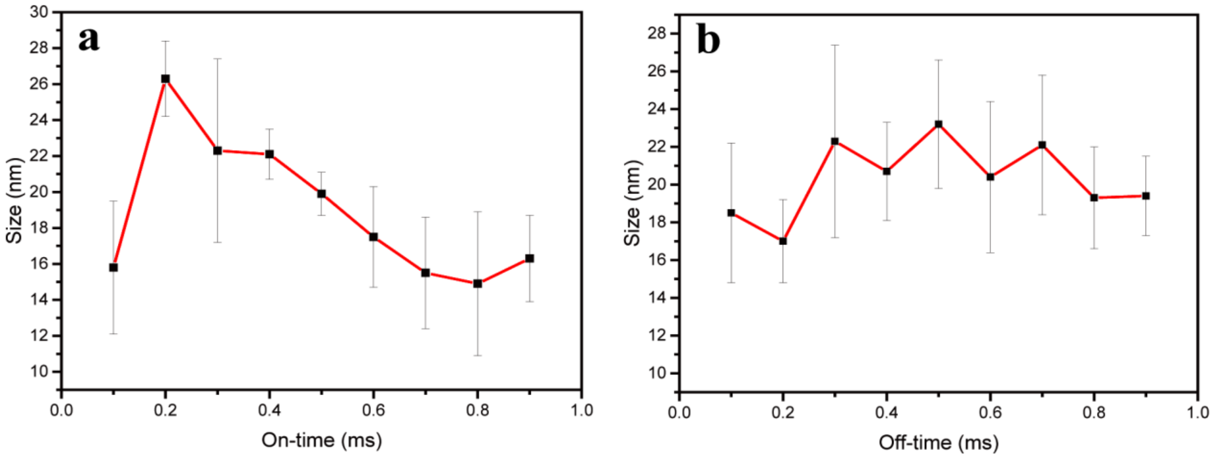

Figure 3. Sizes of AgNPs for varying on-times with the off-time set to 0.3 ms. The peak current was 0.2 A and the PVP concentration was 10 g/L (a). Sizes of AgNPs for varying off-times with the on-time set to 0.3 ms. The peak current was 0.2 A and the PVP concentration was 10 g/L (b).

3.3. Effect of the peak current on the size of AgNPs

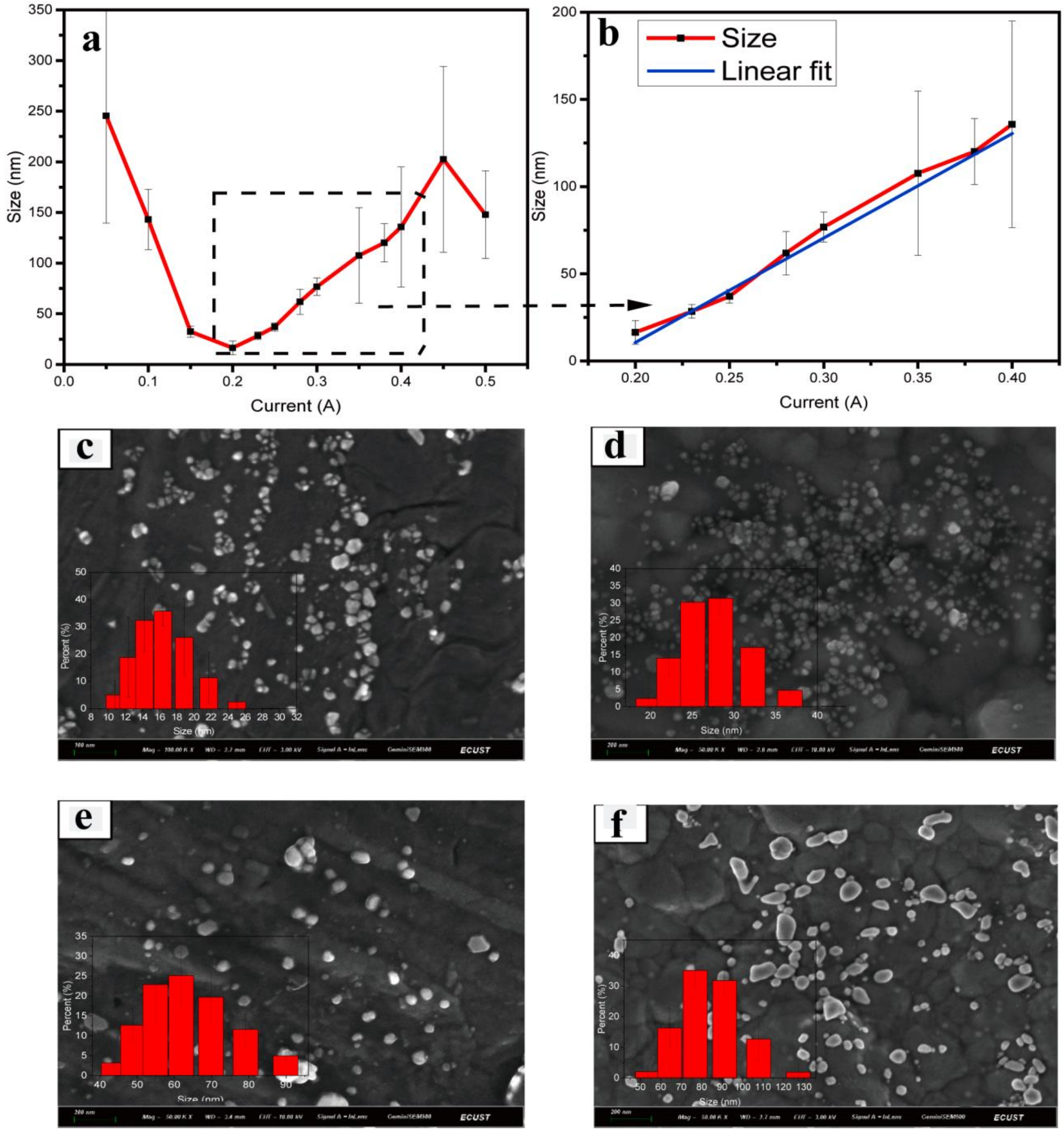

Figure 4. (a) Sizes of AgNPs for varying peak currents with an on-time of 0.9 ms, an off-time of 0.3 ms, and a PVP concentration of 10 g/L. (b) Linear segment of (a), y=598.8x-109.1, r^2=0.9605. FESEM images of silver nanoparticles for varying peak currents, including (c) 0.2 A (d) 0.25 A, (e) 0.28 A and (f) 0.3 A. The magnifications are (c) 10000x and (d), (e) and (f) 5000x.

Figure 4 (a) shows the size of AgNPs for varying peak currents (from 0.05 A to 0.5 A). It can be seen from Figure 4 (a) that the particle size was strongly affected by the current. In this system, when the current was less than 0.2 A, the particle size decreased with increasing current, reaching the smallest size of 16.3±6.8 nm at a current of 0.2 A. The average crystal size of the metal electrodeposits depends on the overpotential, which is influenced by the current density. Therefore, a high current density leads to a high overpotential, and, accordingly, the nucleation rate becomes faster and the quantity of crystal nucleis increase [28, 34]. More crystal nuclei decreased the size of AgNPs, thus the size of AgNPs decreased when the current lower than 0.2 A. However, as shown in Figure 4 (a), with a further increase in the current, the size of the nanoparticles increased as the current was increased from 0.2 A to 0.4 A. The electrodeposition of the nanocrystals was controlled by two factors: the quantity of crystal nuclei and the crystal growth rate [23]. When the peak current was higher than 0.2 A, the formation rate of the crystal nuclei stabilized, and the growth rate of the crystals became the main factor influencing the nanoparticle size, with the high growth rate (due to the high current density) resulting in larger crystals. When the current was greater than 0.4 A, the voltage caused to anodically dissolved and then intermediate Ag^+ formed was reduced to the AgNPs. The size of AgNPs were hard to control due to the as-prepared two kinds of particles in this condition [35, 36]. Therefore, the linear segment from 0.2 A to 0.4 A was chosen to establish a linear regression equation (Figure 4 (b)) to synthesize controllable AgNPs. The line with 8 points was fit to the equation y=598.8x-109.1 by linear regression analysis (y is size of AgNPs in nm and x is the current), with r^2=0.9605. It can be considered that there is a clear linear positive correlation between the size of AgNPs and the peak current. Figure 4 (c-f) shows the FESEM images of the silver nanoparticles when the peak current was 0.2, 0.25, 0.28 and 0.3 A. The sizes were measured with respect to the scale bar, and the values coincided with the data obtained from the Malvern spray analyzer. By comparing the characteristic emission peaks of the silver nanoparticles in the different groups, it can be seen that with increasing current density, the absorption peaks of the silver nanoparticles redshifted to a certain degree. This is due to the larger size of the nanoparticles, which is also consistent with the results of the Malvern particle size analyzer.

4. CONCLUSIONS

A circulation pulsed electrochemical system was successfully established to synthesize well-dispersed and size-controlled spherical AgNPs in the aqueous phase. A solution containing PVP (Polyvinyl Pyrrolidone) was circulated at 6 L/min during the reaction to produce mono-dispersed AgNPs colloids. What's more, the sizes of the AgNPs were affected by the on-time, off-time and peak current in this system. By adjusting the peak current, it was possible to synthesize size-controllable AgNPs (from 16.4±6.8 nm to 135.7±59.19 nm) since there was a clear linear positive correlation between the size of the silver nanoparticles and the peak current. In addition, the present method may be extended to preparing other metal nanoparticles incuding copper, gold and platinum.

ACKNOWLEDGEMENTS
This work was supported by the National Natural Science Foundation of China (NSFC) (21876050), the National key research and development plans of special project for site soils (2018YFC1800600) and the Special Fund from State Key Joint Laboratory of Environment Simulation and Pollution Control (18K10ESPCT).

References

1. B. Jin, A. H. Liu, G.Y. Liu, G.Y. Yang, Z.Z. Zhong , X. Ma, X. Z. Yang , M. Wang, H. Yuan, *Electrochim. Acta*, 90 (2013) 426.
2. J. Yan, H. Tao, M. Zeng, J. Tao, S.H. Zhang, Z.Y. Yan, W. Wang, J.Q. Wang, *Chinese J Catal*., 30 (2009) 856.
3. S. Shende, A. Gade, M. Rai, *Environ Chem Lett*, 15 (2016) 427.
4. P.M. Nia, W.P. Meng, Y. Alias, *Appl. Surf. Sci*., 357 (2015) 1565.
5. C.H. Xue, J. Chen, W. Yin, S.T. Jia, J.Z. Ma, *Appl. Surf. Sci*., 258 (2012) 2468.
6. M. Rycenga, C.M. Cobley, J. Zeng , W. Li , C.H. Moran , Q. Zhang , D. Qin , Y. Xia, *Chem. Rev*., 111 (2011) 3669.
7. B. Sinduja, S.A. John, *Sensor Actuat B-Chem.*, 247 (2017) 648.
8. B. Plowman, S.J. Ippolito, V. Bansal, Y.M. Sabri, A.P. O'Mullane, S.K. Bhargava, *Chem. Commun*., 3 (2009) 5039.
9. D. Long, G. Wu, S. Chen, *Radiat Phys Chem* 76 (2007) 1126.
10. H. Wang, X. Qiao, J. Chen, S.Y. Ding, *Journal of Anhui University of Technology*, 256 (2008): 111.
11. Pietrobon, Brendan, Kitaev, *Chem. Mater*., 20 (2008) 5186.
12. H. Ma, Y. Jiao, B. Yin, S. Wang, S. Zhao, S. Huang, W. Pan, S. Chen, F. Meng, *Chemphyschem*., 5 (2004) 713.
13. O.V. Salata, *J Nanobiotechnol*., 2 (2004) 1.
14. M.L. Rodríguez-Sánchez, M.C. Blanco, L.P.Q. Ma, *J. Phys. Chem*. B, 104 (2000) 9683.
15. R.A. Khahaydarov, R.R. Khaydarov, Gapurova, E. Yuri, S. Thomas, *J. Nanopart. Res*., 11 (2009) 1193.
16. V.V. Le, N.N. Long, S.C. Doanh, Q.T. Bui, *J. Phys. Conf. Ser*., 187 (2009) 012077.
17. J. Reisse, H. Francois, J. Vandercammen, O. Fabre, A. Kirsch-de Mesmaeker, C. Maerschalk, J.L. Delplancke, *Electrochim. Acta*, 39 (1994) 37.
18. V.K. Sharma, R.A. Yngard, Y. Lin, *Adv Colloid Interface Sci.*, 145 (2009) 1.
19. S. Rajawat, M. S. Qureshi, *Arab. J. Sci. Eng*., 39 (2014) 563.
20. N.I. Ikhsan, P. Rameshkumar, N.M. Huang, *Electrochim. Acta*, 192 (2016) 392.
21. Q. Xia, H. Wang, R. Shan, *Ionics*, 24 (2018) 6.
22. Z. Yan, Y. Peng, Y. Wu, J.W. Di, *ChemElectroChem*, 2 (2015) 1072.
23. B. Yin, H. Ma, S. Wang, S. Chen, *J. Phys. Chem*. B, 107 (2003) 8898.
24. Y. Socol, O. Abramson, A. Gedanken, M. Yitzhak, B. Larisa, Z. Arie, *Langmuir.*, 18(2002)4736.
25. J. Zhu , S.T. Aruna , Y. Koltypin , A. Gedanken, *Cheminform.*, 31 (2010) 143.
26. M.T. Reetz, W. Helbig, *J. Am. Chem. Soc.*, 116 (1994) 7401.
27. E.C. Walter, M.P. Zach, F. Favier, B.J. Murray, K. Inazu, J.C. Hemminger, R.M. Penner, *Chemphyschem.*, 4 (2003) 131.
28. M.L. Rodríguez-Sánchez, M.J. Rodríguez, M.C. Blanco, J. Rivas, M.A. López-Quintela, *J. Phys. Chem.* B, 109 (2003) 1183.
29. B. A. Manning, S. R. Kanel, E. Guzman, S. W. Brittle, I. E. Pavel, *J. Nanopart. Res.*, 21 (2019) 213.
30. A. Farzaneh, M. Sarvari, M. Ehteshamzadeh, O. Mermer, *Int. J. Electrochem. Sci.*, 11 (2016) 9676.
31. S. K. Balavandy, K. Shameli, Z. Z. Abidin, *Int. J. Electrochem. Sci.*, 10 (2015) 486.
32. H. Natter, R. empelmann, *Electrochim. Acta*, 49 (2004) 51.
33. H. F. Alesary, A. F. Khudhair, S. Y. Rfaish, H. K. Ismail, *Int. J. Electrochem. Sci.*, 14 (2019) 7116.
34. Y. M. Chai, *Int. J. Electrochem. Sci.*, (2018) 5488.

35. A. M. Funtikov, V.E. Kazarinov, M.I. Urbakh, A. Tadjeddine, *Surf. Sci.*, 239 (1990) 59.
36. L. Rodrıguez-Sanchez, M.C. Blanco, M.A. Lopez-Quintela, *J. Phys. Chem. B*, 104 (2000) 9683.